



miR-654-5p Contributes to the Activation and Proliferation of Hepatic Stellate Cells by Targeting RXR α

Heming Ma¹, Xiaomei Wang¹, Xu Liu¹, Chang Wang¹, Xiuzhu Gao^{1*} and Junqi Niu^{1,2*}

¹Department of Hepatology, The First Hospital of Jilin University, Changchun, China, ²Key Laboratory of Organ Regeneration and Transplantation of Ministry of Education, The First Hospital of Jilin University, Changchun, China

OPEN ACCESS

Edited by:

Xiaodong Zhao,
Shanghai Jiao Tong University, China

Reviewed by:

Liya Pi,
Tulane University, United States
Zheng Jin,
Shenzhen University, China

*Correspondence:

Xiuzhu Gao
xiuzhugao@jlu.edu.cn
Junqi Niu
junqiniu@jlu.edu.cn

Specialty section:

This article was submitted to
Signaling,
a section of the journal
Frontiers in Cell and Developmental
Biology

Received: 22 December 2021

Accepted: 22 March 2022

Published: 06 April 2022

Citation:

Ma H, Wang X, Liu X, Wang C, Gao X
and Niu J (2022) miR-654-5p
Contributes to the Activation and
Proliferation of Hepatic Stellate Cells by
Targeting RXR α .
Front. Cell Dev. Biol. 10:841248.
doi: 10.3389/fcell.2022.841248

Liver fibrosis (LF) is a major disease that threatens human health. Hepatic stellate cells (HSCs) contribute directly to LF via extracellular matrix (ECM) secretion. Moreover, RXR α is an important nuclear receptor that plays a key regulatory role in HSC activation. Meanwhile, microRNAs (miRNAs) have been identified as significant regulators of LF development. In particular, miR-654-5p is involved in cellular migration and proliferation, and *via* bioinformatics analysis, has been identified as a potential factor that targets RXR α in humans and in mice. However, the precise relationship between miR-654-5p and RXR α in the context of LF, remains unknown and is the primary focus of the current study. To establish *in vitro* activated cell model human primary HSCs were cultured *in vitro* and LX-2 cells were stimulated with recombinant human TGF- β 1. mRNA and protein levels of RXR α , miR-654-5p and fibrogenic genes were compared in quiescent and activated HSCs. Moreover, after transfected with miR-654-5p mimics, the expression changes of above related genes in LX-2 cells were estimated. Meanwhile, cell proliferation and apoptosis were detected in miR-654-5p overexpressed LX-2 cells. Simultaneously, the targeted binding between miR-654-5p and RXR α was verified in LX-2 cells. Carbon tetrachloride (CCl₄)-induced mouse model with liver fibrosis was use to research the role of the miR-654-5p *in vitro*. Our results show that miR-654-5p expression levels increased in activated human HSCs and TGF β -treated LX-2 cells. Moreover, miR-654-5p mimics markedly promoted LX-2 cell proliferation while inhibiting their apoptosis. Accordingly, the expression levels of RXR α are decreased in activated HSCs and LX-2 cells. Additionally, dual-luciferase reporter assay results reveal direct targeting of RXR α by miR-654-5p. Similarly, *in vivo* miR-654-5p overexpression aggravates LF in mice that are intraperitoneally injected with CCl₄. Taken together, our findings elucidated a novel molecular mechanism with potential use for treatment of LF.

Keywords: RXR α , miR-654-5p, hepatic stellate cells, liver fibrosis, target

INTRODUCTION

Liver fibrosis (LF) is a dynamic and reversible pathological process. Uncontrolled LF progresses to cirrhosis and even hepatocellular carcinoma (HCC), a major disease threatening human health (Tao et al., 2020). LF is characterized by extracellular matrix (ECM) accumulation, a process that is closely associated with hepatic stellate cells (HSCs). Transdifferentiation of quiescent HSCs into a myofibroblast-like cells is referred to as “activation” (Tsuchida and Friedman, 2017). In fibrotic

livers, activated HSCs can proliferate, migrate, and contract, while also secreting a large amount of ECM, tissue inhibitors of metalloproteinases (TIMPs), and matrix metalloproteinases (MMPs), all of which play key roles in LF (Ezhilarasan et al., 2018; Roeb, 2018). Hence, maintenance of HSC quiescence may serve to resolve LF.

MicroRNAs (miRNAs) are ~22 nt long, single-stranded small non-coding RNAs that regulate various cellular biological processes, including cell proliferation, apoptosis, and differentiation (Tsai and Yu, 2010). As such have summarized several miRNAs involved in the regulation of LF through HSCs (Ezhilarasan, 2020; Fang et al., 2021). In particular, microRNA-654-5p (miR-654-5p) is involved in autophagy and inflammatory signaling pathways (Kong, 2020; Li et al., 2021a; Wang et al., 2021) and regulates the proliferation and migration of various tumor cells (Tan et al., 2016; Lu et al., 2018; Huang et al., 2020; Xu et al., 2020; Zhang et al., 2020). Meanwhile, inhibition of the miR-654-5p/SMAD2 axis induces HCC cell proliferation, invasion, and migration (Lu et al., 2021). However, the role of miR-654-5p in HSC activation within the context of LF, as well as the underlying potential molecular mechanism remain to be elucidated.

Retinoic acid (RA), the main active metabolite of vitamin A, has a key role in several essential biological processes, including embryogenesis, organogenesis, cell proliferation, differentiation, and apoptosis. The biological effects of RA are primarily mediated by retinoid receptors (RRs), including retinoid acid receptors (RARs) and retinoid X receptors (RXRs). RRs regulate gene transcription after binding to retinoic acid response elements (RAREs) in the target gene promoter region (Abdel-Bakky et al., 2020; Li et al., 2021b). RRs are expressed in quiescent HSCs in rodents and humans. RXRs have three subtypes: RXR- α , - β , and - γ , of which RXR α is the most expressed subtype on HSCs. However, the expression of RXR α decreases following HSC activation (Vogel et al., 2000). Specifically, bioinformatics analysis demonstrated that RXR α expression is downregulated in the livers of patients with liver cirrhosis caused by hepatitis B virus (HBV), hepatitis C virus, and nonalcoholic fatty liver disease (NAFLD), and is also downregulated in HSCs that are activated *in vivo* in carbon tetrachloride (CCl₄)-induced LF mice (He et al., 2020). Consistent with this, downregulation of RXR α mRNA has also been reported during activation of HSCs in rats with advanced LF induced by bile duct ligation and CCl₄. In contrast, overexpression of RXR α in HSCs *in vitro* can inhibit the secretion of α -smooth muscle actin (α -SMA) and collagen I in HSCs, while *in vivo* overexpression of RXR α could resolve LF in mice, suggesting that this nuclear receptor plays a key role in the activation of HSCs and in LF (Ohata et al., 1997; Wang et al., 2011). Indeed, our previous RNA-seq study reported that miR-654-5p expression is significantly upregulated, while RXR α expression is downregulated in culture-activated human primary HSCs *in vitro* (Supplementary Figure S1). Therefore, in the current study, we hypothesized that miR-654-5p participates in the activation and proliferation of HSCs through the negative regulation of RXR α , thereby promoting LF.

MATERIALS AND METHODS

Isolation of Primary Human HSCs, Cell Culture and Stimulation

Liver tissues were obtained intraoperatively from patients undergoing orthotopic liver transplantation or surgical liver resection for primary biliary cirrhosis, primary sclerosing cholangitis, and HBV-related cirrhosis. Demographic and clinical characteristics, laboratory indices, and disease statuses of the patients are shown in **Supplementary Table S1**. The distance from the obtained liver tissue to the edge of the lesion was at least 5 cm. Written informed consent was obtained from the patients for use of their tissues for research purposes, according to the ethical guidelines of the First Hospital of Jilin University (NO. 2019-356). Subsequently, primary human HSCs were isolated from the wedge sections of human livers using the density gradient centrifugation method (Werner et al., 2015). In brief, collagenase IV (Sigma-Aldrich, St. Louis, MO, United States) was used to perfuse and digest the liver tissue, and a hepatic cell suspension was obtained after blunt separation. Primary hepatocytes (HCs) were separated after centrifugation at 50 g for 5 min, and the supernatant was further centrifuged at 500 g for 5 min at 4°C. Using 8.5% Optiprep gradient medium (Stemcell, Vancouver, Canada), we removed other non-parenchymal cells, including liver sinusoidal endothelial cells and Kupffer cells. Primary HSCs, and the human immortalized hepatic stellate cell line (LX-2) (kindly provided by Dr. Zhengkun Tu) were maintained in Dulbecco's modified eagle's medium (DMEM; Gibco, Waltham, MA, United States) supplemented with 10% fetal bovine serum (FBS; Gibco). For TGF β 1-induced activation, LX-2 cells were treated with TGF- β 1 (5 ng/ μ L; R&D, United States) for 24 h after starvation. The cells were then incubated in a 5% CO₂ incubator at 37°C.

Immunofluorescence Staining

HSCs were fixed with 4% paraformaldehyde (Solarbio, Beijing, China) for 15 min at room temperature (25°C), washed with phosphate-buffered saline (PBS), and subsequently blocked with 2% bovine serum albumin for 30 min. HSCs were then incubated for 2 h at 37°C with a primary monoclonal anti- α -SMA antibody (1:200 dilution; Abcam, Cambridge, MA). After washing with PBS, the cells were incubated for 1 h at room temperature with a secondary polyclonal goat anti-rabbit IgG (H + L; 1:200; Earthox, San Francisco, United States). The negative control was obtained by not using the primary antibodies. After incubation with the above antibodies, cells were washed with PBS and counterstained with 4,6-diamidino-2-phenylindole (DAPI; Invitrogen, Carlsbad, CA, United States) for 3 min. Immunofluorescence staining was detected and photographed using a laser scanning microscope (Axiovert 100M; Zeiss, Jena, Germany) at 200 \times magnification.

Histological Analyses

Mouse liver tissue sections were cut into 3 μ m silces, and embedded in paraffin. Collagen deposition in liver tissue sections was localized using standard histological techniques with Masson's trichrome staining. Each section was assessed

under a light microscopic and photographed at 40 \times magnification.

Animals

Male C57BL/6 mice (6 weeks old) were purchased from Charles River (Beijing, China). All mice were fed a standard rat chow diet and housed under a 12 h light/dark cycle. After acclimatization for 7 days, the mice were randomly divided into four groups: negative control (NC; n = 6), CCl₄ group (n = 6), CCl₄+AAV-NC group (n = 7), and CCl₄+AAV-miR-654-5p group (n = 7). Adeno-associated virus serotype 8 (AAV8) particles encoding miR-654-5p (hereafter referred to as AAV-miR-654-5p) and control AAV particles (AAV-NC) were purchased from Hanbio, Shanghai, China, and were administered to the CCl₄+AAV-miR-654-5p and CCl₄+AAV-NC groups at a dose of 3×10^{11} viral genomes (vg) per animal *via* tail vein injection. After 1 week, the mice in the CCl₄, CCl₄+AAV-NC, and CCl₄+AAV-miR-654-5p groups were intraperitoneally injected with a 10% CCl₄ (Aladdin, China) dose at 1 ml/kg (diluted with edible olive oil before injection) three times per week. Mice in the NC group were similarly administered the same solvent. After 6 weeks, the mice were sacrificed, and their liver tissues were dissected. Blood samples were centrifuged, and serum was stored at -80°C . Additionally, a portion of the liver tissue samples were fixed in 4% formaldehyde, while the remaining sample was stored at -80°C until use. All experiments involving mice were conducted in accordance with the ethical guidelines of the Animal Ethics Committee of First Hospital of Jilin University (Approval NO. 20220002).

Transient Transfection

Cells were transfected with 50 nM miR-654-5p mimics or mimics-NC (RiboBio, Guangzhou, China) using Lipofectamine 3,000 (Invitrogen) following the manufacturer's protocol. Similarly, cells were transfected with pcDNA3.1-RXR α plasmid or its control plasmid pcDNA3.1-NC (Sangon Biotech).

Western Blot Assay

Cells were lysed in RIPA buffer (Beyotime, Shanghai, China) containing PMSF (Solarbio). This assay was performed using standard western blotting techniques with the following primary antibodies: anti-RXR α (Abcam), anti-collagen I (Proteintech, Chicago, United States), anti-MMP2 (Proteintech) and anti-tubulin (YTHX Biotechnology, Beijing, China).

Quantitative Reverse-transcription Polymerase Chain Reaction (qRT-PCR)

Total RNA was extracted from the cells/liver tissues using EastepTM Total RNA Extraction Kit (Promega, Madison, United States) and miRNAs were extracted from the cells/liver tissues using the EasyPure miRNA Kit (TransGen, Beijing, China) following the manufacturer's instructions. Complementary DNA (cDNA) was synthesized using TransScript One-Step gDNA Removal and cDNA Synthesis

SuperMix (TransGen) to detect mRNA. cDNA was generated using a Ribo SCRIPTTM Reverse Transcription kit (RiboBio) to detect miRNA. Quantitative real-time polymerase chain reaction (qRT-PCR) was performed using PerfectStartTM Green qPCR SuperMix (TransGen). β -actin was used as an mRNA control. U6 was used as a reference miRNA control. The primers for U6/miR-654-5p were obtained from RiboBio Co., Ltd. All other qPCR primers used are listed in **Table 1** qPCR was performed using the Agilent Mx3005P Real-Time PCR System (Applied Biosystems, Foster City, CA).

Luciferase Reporter Assay

The wild-type (WT) or mutant (MUT) RXR α 3' UTR was synthesized and subcloned into the pmirGLO Dual-Luciferase miRNA Target Expression Vector (Promega). HEK293 cells were co-transfected with miR-654-5p mimics and pGLO-WT-RXR α or pGLO-MUT-RXR α using Lipofectamine 3,000. Luciferase activity was measured 48 h after the co-transfection using the Dual-Luciferase Reporter Assay System (Promega) following the manufacturer's instructions. Relative luciferase activity was calculated by normalizing firefly luciferase activity to Renilla luciferase activity.

Cell Counting Kit-8 (CCK-8) Assay

LX-2 cells were seeded into 96-well plates (3,000 cells/well) and cultured in serum-free DMEM after transfection; the medium was replaced every 48 h. CCK-8 solution (10 μL ; Beyotime, Shanghai, China) was added to each well at 24, 48, 72, 96, 120, 144, and 168 h after transfection, respectively. Absorbance was measured at 450 nm using a microplate reader (Thermo Fisher Scientific, Waltham, MA, United States).

Flow Cytometry Analysis

To detect cell apoptosis, LX-2 cells were cultured in serum-free DMEM for 5 days after transfection to induce apoptosis by starvation. Trypsin was used to digest the cells for flow cytometry analysis. Cell apoptosis was measured by staining cells with PE Annexin V and 7-AAD using a PE Annexin V Apoptosis Detection Kit (BD Biosciences, Franklin Lakes, NJ, United States) for 15 min at room temperature in the dark. Apoptosis was detected using a FACS Canto flow cytometer (BD).

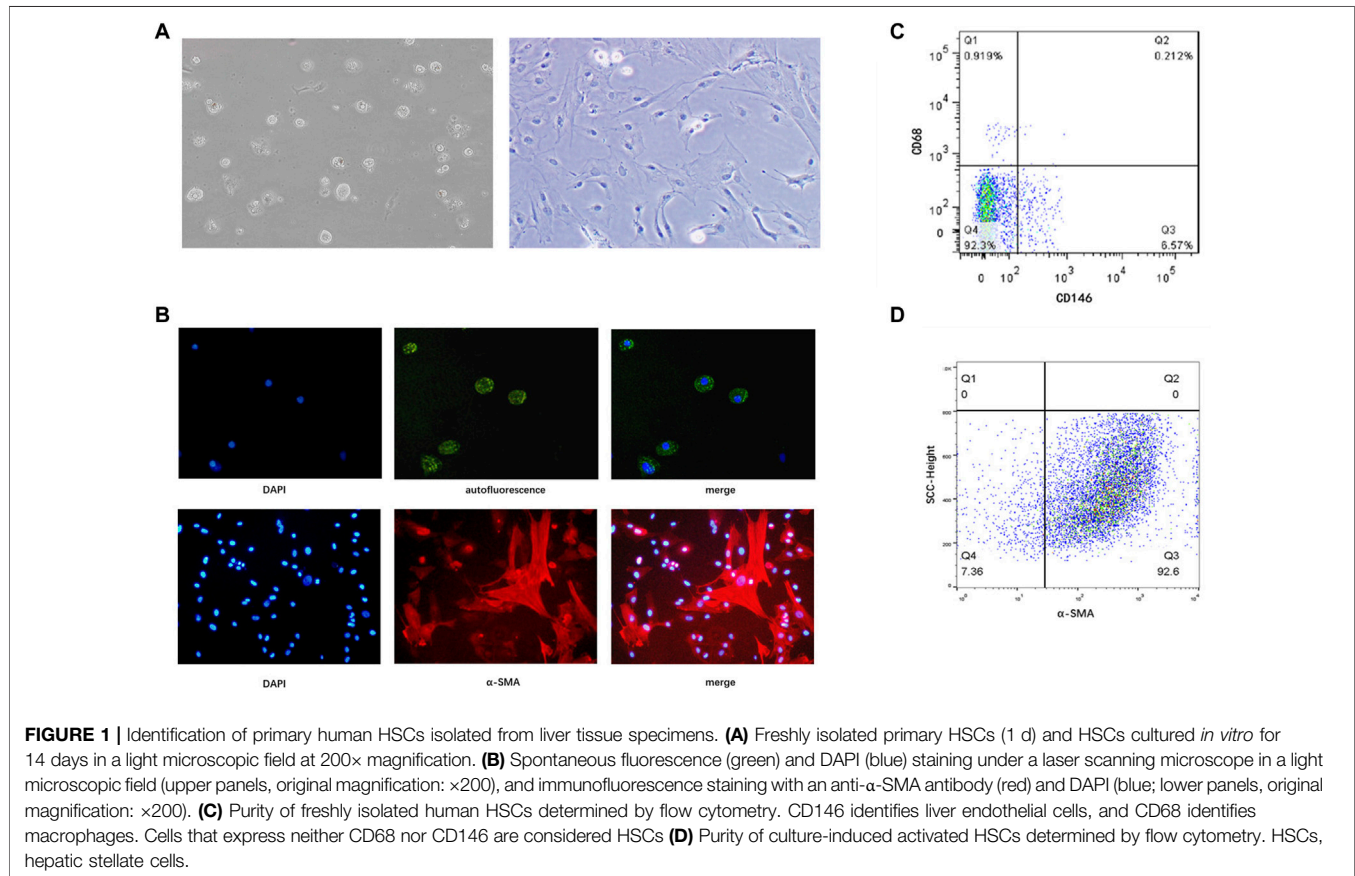
To detect the purity of isolated HSCs, freshly isolated HSCs were washed and counted. They were then incubated with CD68 and CD146 antibodies (BD Biosciences, San Jose, CA) in the dark at room temperature for 30 min. In addition, other HSCs were cultured *in vitro* for 14 days and then collected. After washing, cells were fixed and permeabilized with the BD Cytofix/CytopermTM Fixation/Permeabilization kit (BD) according to the manufacturer's introductions. Fixed cells were further incubated with an α -SMA antibody (R&D). After washing, labeled cells were resuspended and analyzed by flow cytometry. Flowjo was used to analyze the flow data.

ALT, AST and Hydroxyproline Measurements

The levels of serum alanine aminotransferase (ALT), aspartate aminotransferase (AST) and hydroxyproline (Hyp) were

TABLE 1 | Primers used for the real-time polymerase chain reaction.

Genes	Forward (5'-3')	Reverse (5'-3')
has- β -actin	CACCATTGGCAATGAGCGGTTTC	AGGTCCTTTGCGGATGTCCACGT
has-col1 α 1	GAGGGCCAAGACGAAGACATC	CAGATCAGTCATCGCACAAAC
has-MMP2	AGCGAGTGGATGCCGCTTTAA	CATTCCAGGCATCTGCGATGAG
has- α -SMA	CTATGCCTCTGGACGCACAAC	CAGATCCAGACGCATGATGGCA
has-RXR α	TTGCCAAGCAGCCGACAAACAG	AAGGAGGCGATGAGCAGCTCAT
mmu-col1 α 1	CCTCAGGGTATTGCTGGACAAC	CAGAAGGACCTTGTGGCCAGG
mmu- α -SMA	TGCTGACAGAGGCCACCACTGAA	CAGTTGTACGTCAGAGGCATAG
mmu-MMP2	CAAGGATGGAATCCTGGACAT	TACTCGCCATCAGCGTTCCCAT
mmu-RXR α	GTGAAAGATGGGATTCTCCTGGC	GTACGCATCTTAGACACCAGC



measured in the mice using ALT, AST and Hyp measuring reagent kits (Nanjingjiancheng, Nanjing, China) according to the manufacturer's instructions.

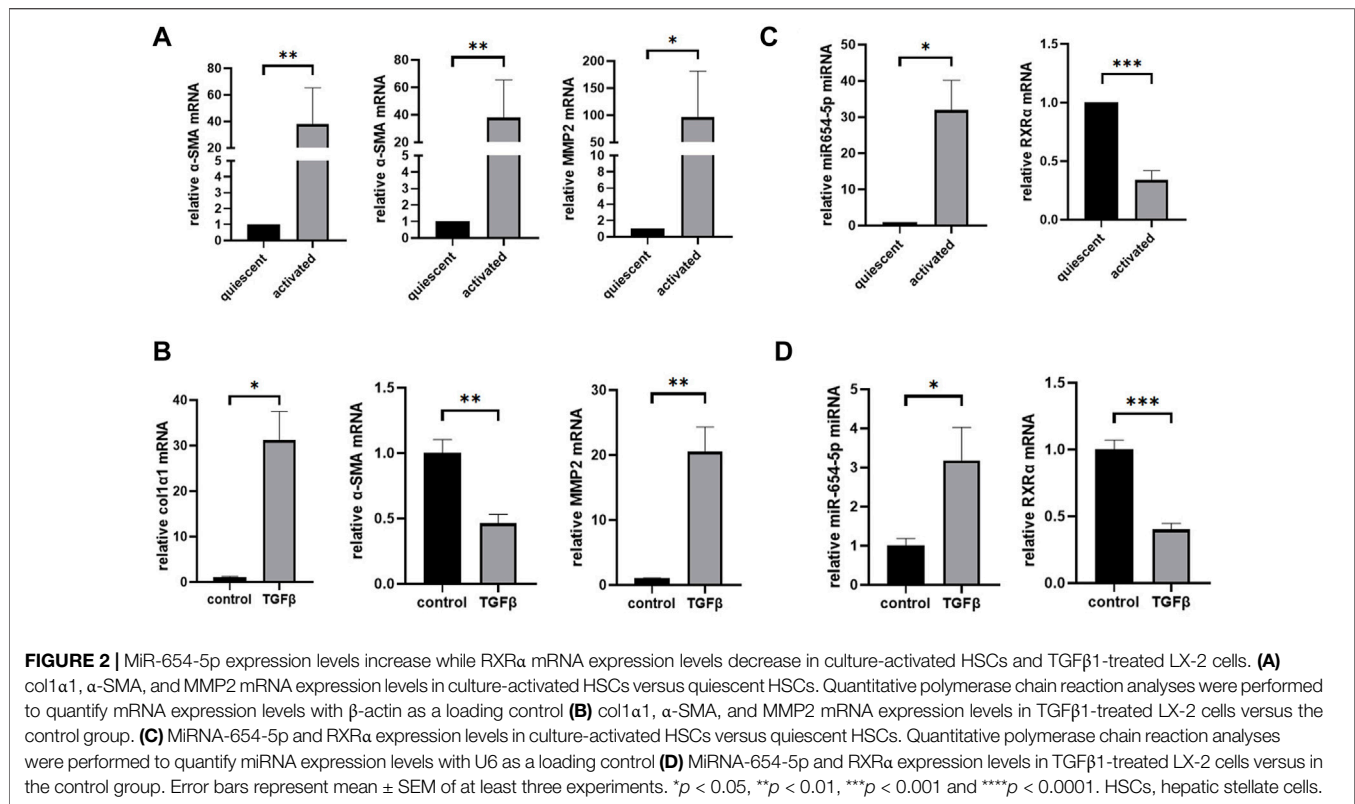
Statistical Analysis

Data are presented as mean \pm standard deviation (SD) of at least three independent experiments. The paired *t*-test was used to analyze the differences in mRNA or miRNA expression from qRT-PCR results, and $*p < 0.05$, $**p < 0.01$, $***p < 0.001$, and $****p < 0.0001$ from Prism 8.0.1 software (GraphPad Software, San Diego, CA) were defined as statistically significant.

RESULTS

Identification of Isolated HSCs

Although there are no known specific markers for quiescent human HSCs, these cells store several cytoplasmic retinoid droplets rich in vitamin A. Therefore, we detected spontaneous fluorescence of these lipid droplets in freshly separated (1 d) HSCs. HSCs were cultured in plastic dishes for 14 days to induce spontaneous cellular activation. The activated HSCs underwent morphological changes and expressed α -SMA (**Figures 1A,B**). Moreover, since HSCs are similar in size to liver endothelial cells and macrophages, it is likely that the layer obtained following density gradient



centrifugation contained all three of these cell subsets. Therefore, we identified liver endothelial cells *via* CD146 and macrophages *via* CD68. The remaining CD68⁻ CD146⁻ cells were considered to be HSCs. The results showed that the purity of freshly isolated HSCs was >90% (**Figure 1C**). Subsequently, we labeled HSCs with α -SMA and analyzed them *via* flow cytometry, confirming that the purity of isolated HSCs was >90% (**Figure 1D**).

MiR-654-5p is Significantly Upregulated While RXR α is Downregulated During Natural Activation of HSCs and in TGF- β 1-Treated LX-2 Cells

To confirm the spontaneous activation of HSCs following *in vitro* culture, the expression levels of activation-related genes in HSCs were measured. After 14 days of *in vitro* culture, the mRNA expression levels of collagen type 1- α 1 (col1 α 1), α -SMA, and matrix metalloproteinase 2 (MMP2) were significantly upregulated compared to those at on day 1 (**Figure 2A**). Similarly, after 48 h of TGF β 1 stimulation, the mRNA expression levels of col1 α 1 and MMP2 in LX-2 cells were significantly upregulated, while that of α -SMA decreased (**Figure 2B**). After *in vitro* culturing for 14 days, miR-654-5p and RXR α expression was evaluated in activated primary HSCs. Our results showed that the relative expression of miR-654-5p was significantly increased in activated HSCs compared to quiescent HSCs (freshly isolated; p < 0.05), while the relative expression of RXR α decreased (p < 0.001; **Figure 2C**). In addition, we treated LX-2 cells with TGF- β 1, an HSCs activator. A similar

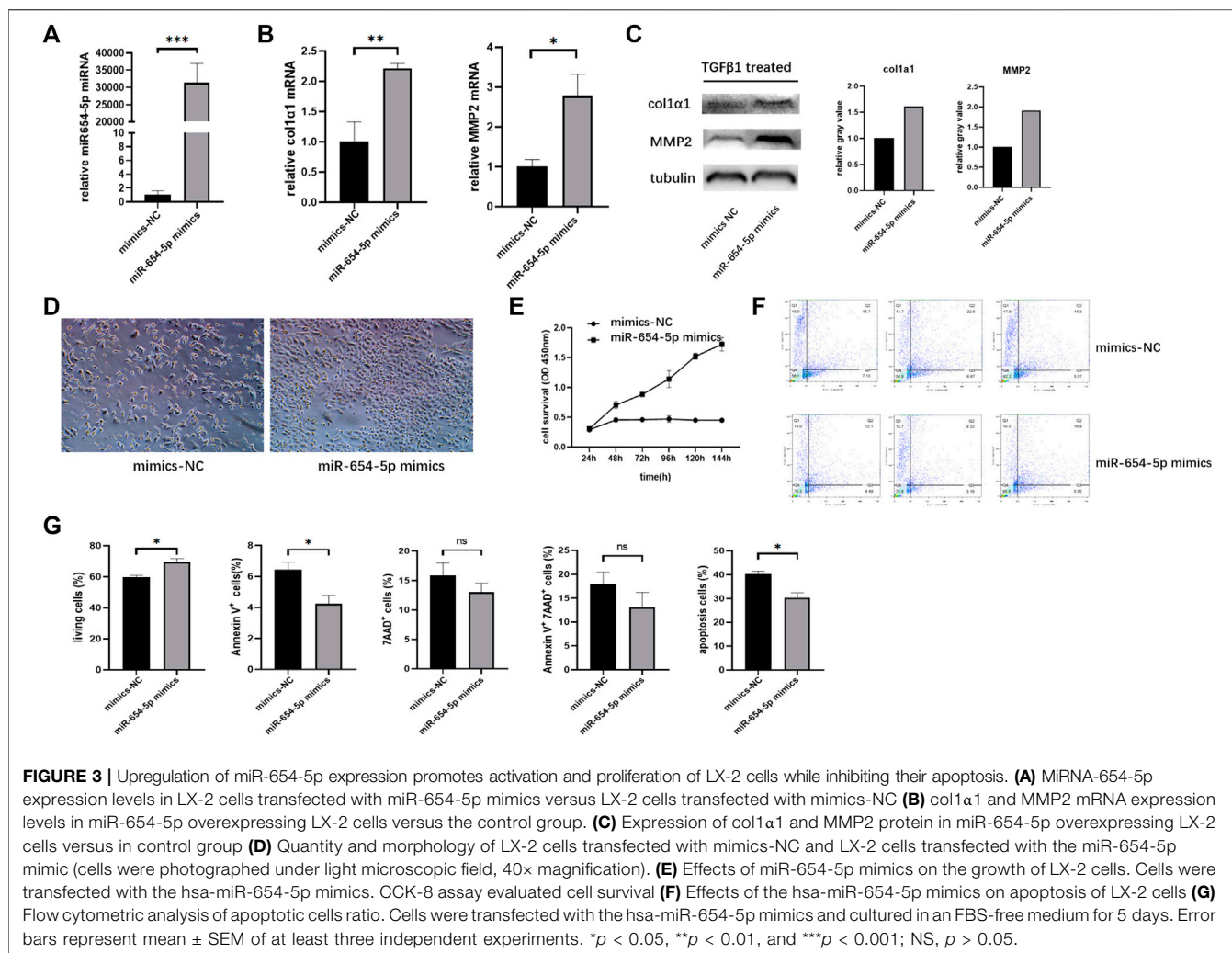
trend was observed in TGF- β -induced LX-2 cells compared to the NC group (p < 0.05 and p < 0.001, respectively; **Figure 2D**).

Upregulation of miR-654-5p Promotes Activation and Proliferation of LX-2 Cells While Inhibiting Their Apoptosis

To explore the function of miR-654-5p in LF, we modulated the expression of miR-654-5p by transfecting LX-2 cells with mimics. First, we overexpressed miR-654-5p in LX-2 cells by transfection with miR-654-5p mimics (**Figure 3A**) and found that overexpression of miR-654-5p promoted the mRNA expression levels of HSC activation markers col1 α 1 and MMP2 compared to the control group (mimics-NC; **Figure 3B**; p < 0.01 and p < 0.05). Subsequently, LX-2 cells were treated with TGF β 1 after miR-654-5p mimics/mimics-NC transfection. The resulting expression levels of col1 α 1 and MMP2 proteins were increased in miR-654-5p-overexpressing LX-2 cells (**Figure 3C**). These results validated the functional relevance of miR-654-5p in the activation of HSCs *in vitro*.

LX-2 cells transfected with the miR-654-5p mimic were then starved in an FBS-free medium for 5 days. The resulting quantity and morphology of LX-2 cells differed from those of the NC group (**Figure 3D**). Moreover, the CCK-8 assay results showed that overexpression of miR-654-5p significantly promoted the proliferation of LX-2 cells (**Figure 3E**).

In addition, flow cytometry analysis results suggested that LX-2 cells treated with the miR-654-5p mimic exhibited changes in apoptosis compared to mimic-NC. Specifically, three repeated



experiments showed that Annexin V-positive cells were significantly increased after miR-654-5p transfection; therefore, miR-654-5p reduced early apoptosis of LX-2 cells (Figures 3F,G). Overall, these results indicate that upregulation of miR-654-5p promotes the activation and proliferation of HSCs while inhibiting apoptosis.

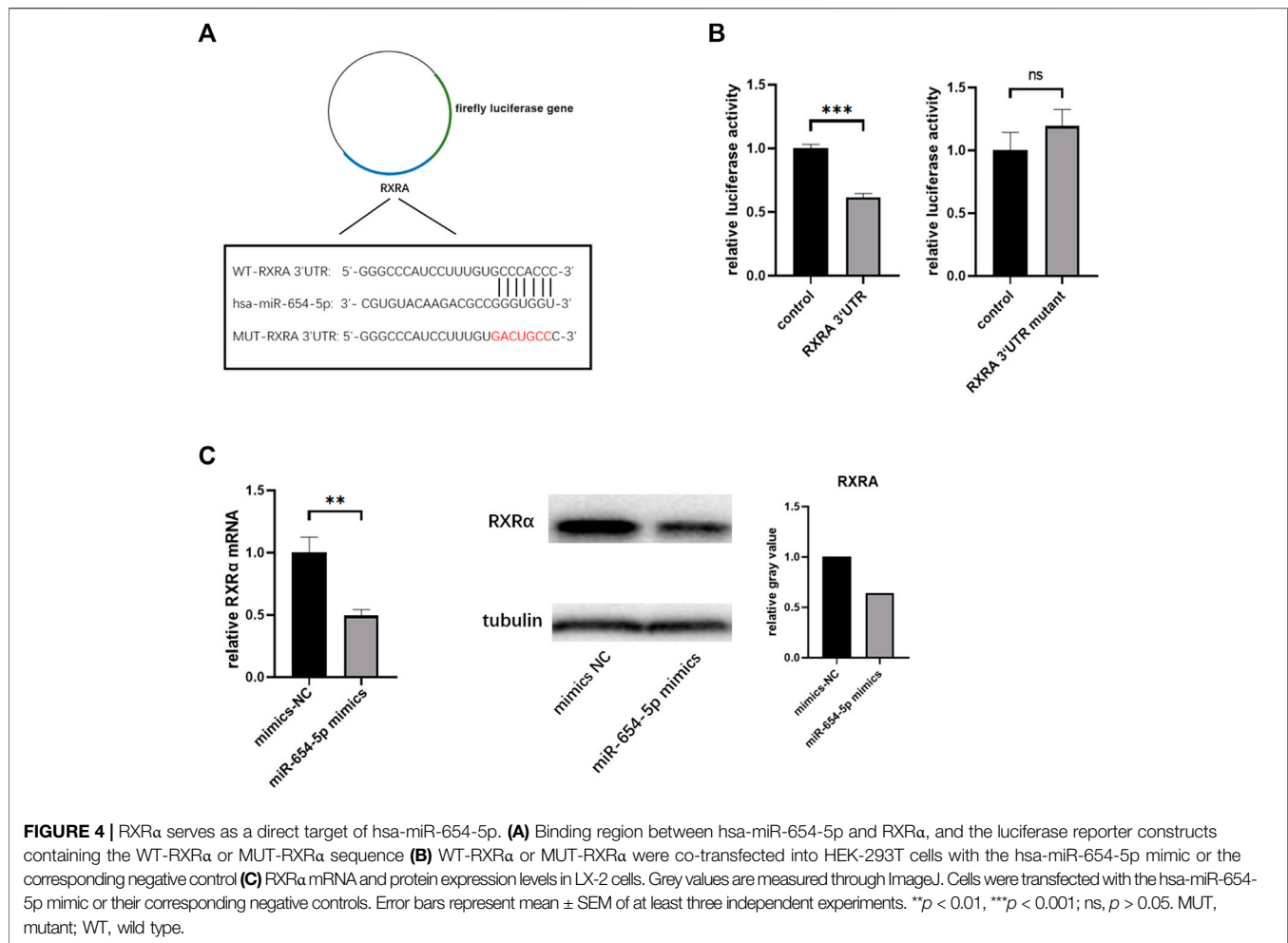
MiR-654-5p Directly Targets RXR α

To identify the potential mRNAs targeted by miR-654-5p, bioinformatics analysis using TargetScan (http://www.targetscan.org/vert_71/) and miRwalk (<http://mirwalk.umm.uni-heidelberg.de/>) databases were carried out. Based on our lab RNA-seq data from the previous period, RXR α was noted to be a candidate involved in miR-654-5p regulation of HSCs. The speculative binding region between hsa-miR-654-5p and RXR α , based on TargetScan results, is shown in **Supplementary Figure S2**. A dual-luciferase reporter assay was then used to validate the association between the two. To this end, luciferase reporter plasmids of WT-RXR α - and MUT-RXR α 3' UTR were constructed and are shown in **Figure 4A**. Co-transfection of the luciferase reporter plasmid containing WT-RXR α with miR-654-5p mimics in HEK-293T cells decreased reporter activity.

Conversely, the luciferase reporter plasmid co-transfection containing MUT-RXR α with miR-654-5p mimics did not alter the luciferase activity (**Figure 4B**). In addition, the levels of both RXR α mRNA and protein were markedly inhibited by miR-654-5p upregulation in LX-2 cells (**Figure 4C**). These findings indicate that miR-654-5p directly targets RXR α .

RXR α Overexpression Rescues the Effect of miR-654-5p on LX-2 Cells

To verify that miR-654-5p regulates the activation, proliferation and apoptosis of HSCs by targeting RXR α , we transfected LX-2 cells with pcDNA3.1-RXR α plasmid to ectopically overexpress RXR α and confirmed the elevated levels of RXR α (**Figure 5A**), LX-2 cells were then co-transfected with miR-654-5p mimics and pcDNA3.1-RXR α /pcDNA3.1-NC. Subsequently, the transfected cells were treated with TGF β 1 to induce col1 α 1 expression. The results of western blotting showed that the overexpression of RXR α suppress the miR-654-5p mimics-induced expression of col1 α 1 protein (**Figure 5B**).

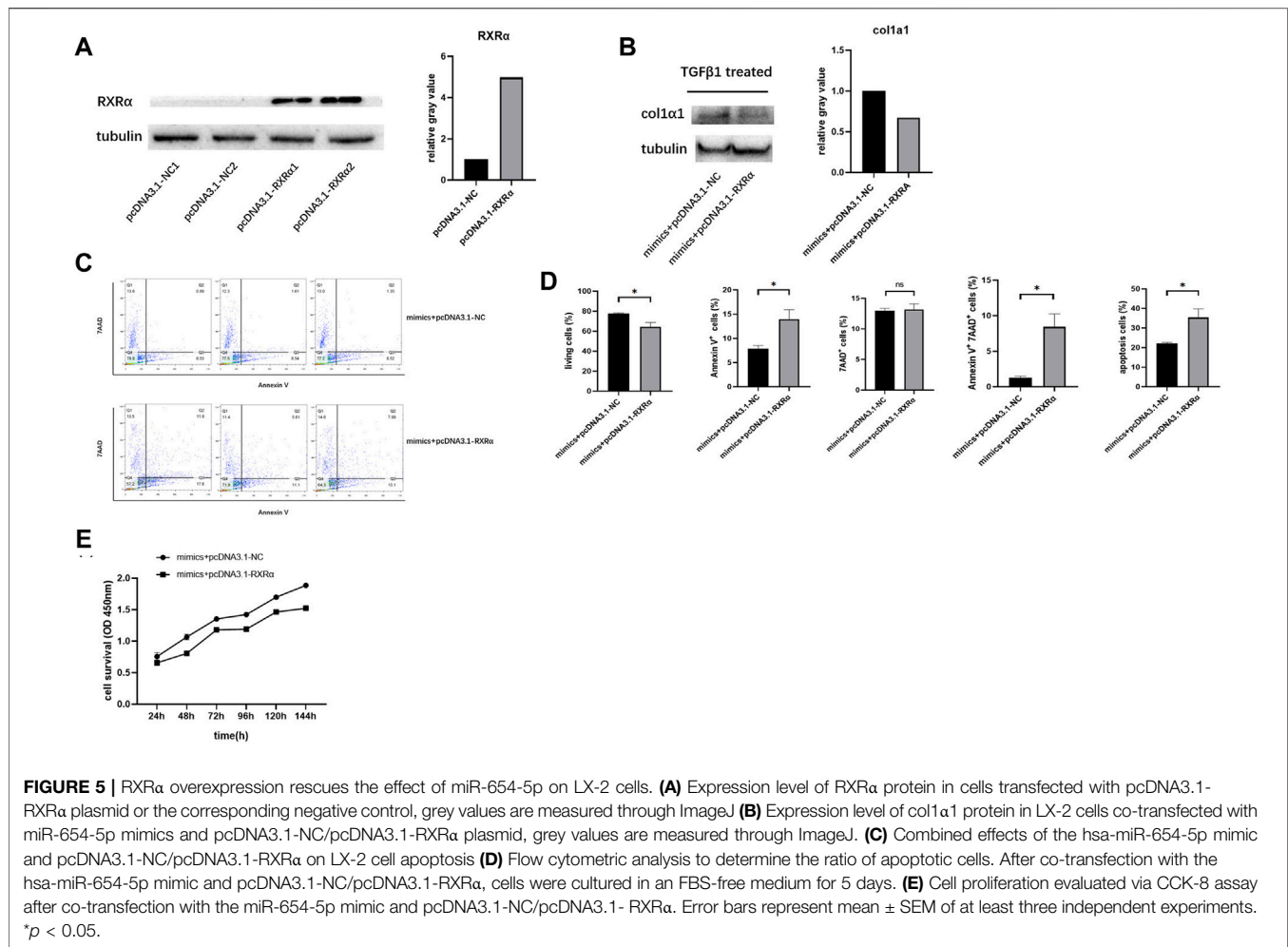


The co-transfected cells were also obtained to assess apoptosis using flow cytometry analysis. Results showed that following co-transfection with pcDNA3.1-RXR α and miR-654-5p mimics, the proportion of LX-2 cells undergoing early apoptosis had increased compared to those transfected with pcDNA3.1-NC and miR-654-5p mimics (Figures 5C,D). Similarly, CCK-8 assay results showed a decline in the proliferation in cells co-transfected with pcDNA3.1-RXR α and miR-654-5p mimics (Figure 5E).

MiR-654-5p Is Increased in CCl₄-Induced LF, and miR-654-5p Overexpression Aggravates LF in Mice

To further investigate the role of miR-654-5p *in vivo*, we established a CCl₄-induced LF mouse model. The mRNA levels of α -SMA, coll1a1, and MMP2, were higher in the livers of CCl₄-treated mice than in those of control mice (Figure 6A). Masson's trichrome staining further revealed increased ECM deposition in the livers of CCl₄-treated mice compared to those of control mice. In addition, Hyp content was upregulated in the liver tissues of mice treated with CCl₄ (Figure 6B). These results confirmed that CCl₄ induced LF in the mouse model.

Subsequently, the levels of mmu-miR-654-5p and mmu-RXR α between the CCl₄ model and NC groups were estimated. Results showed that mmu-miR-654-5p expression was upregulated in fibrotic mouse, while mmu-RXR α mRNA level was consistently downregulated (Figure 6C). The targeting relationship between mmu-miR-654-5p and mmu-RXR α was then predicted using TargetScan (Supplementary Figure S3). To assess the delivery of AAV into the liver, the level of miR-654-5p was quantified in mouse livers by qRT-PCR analysis. Expression of miR-654-5p was significantly upregulated in the CCl₄+AAV-miR-654-5p group compared to that in the CCl₄+AAV-NC group. Consistent with this, the mRNA expression of RXR α was decreased (Figure 6D). In addition, serum ALT and AST levels were compared between the CCl₄+AAV-miR-654-5p and CCl₄+AAV-NC groups. No significant differences were observed in AST and ALT content levels between the two groups (Figure 6E). Finally, we also observed a significant increase in fibrosis within AAV-miR-654-5p overexpressing livers, as evidenced by increased collagen deposition in the liver, detected *via* Masson's trichrome staining, and increased Hyp levels (Figure 6F).



DISCUSSION

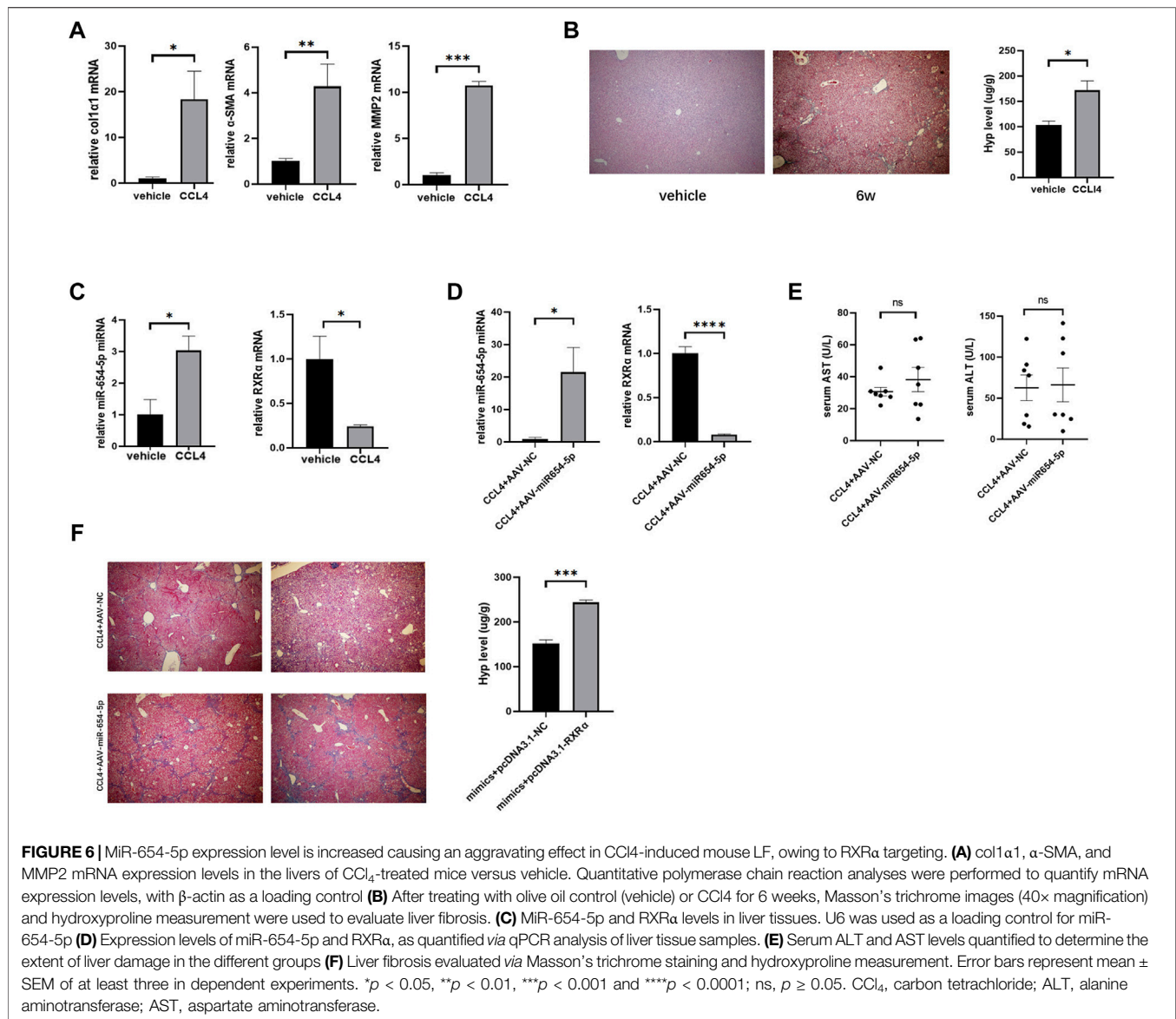
In the current study, our findings showed that miR-654-5p expression was upregulated in culture-induced activated human primary HSCs and TGF- β 1-stimulated LX-2 cells, suggesting that miR-654-5p is, at least partially, involved in LF development. Furthermore, transfection of cells with the miR-654-5p mimic significantly induced ECM synthesis, upregulated col1 α 1 expression, and promoted HSC proliferation, while inhibiting the apoptosis of HSCs. In addition, we found that miR-654-5p regulates profibrotic genes expression and cellular biological functions through RXR α .

LF is characterized by excessive deposition of ECM components, in particular type I collagen (Bataller and Brenner, 2005; Friedman, 2008). HSCs convert from a resting to active phenotype and migrate to the damaged area where they produce ECM after liver injury (Tsuchida and Friedman, 2017). Meanwhile, MMPs regulate liver matrix degradation, with MMP2 defined as one of the most relevant MMPs for degrading the normal liver matrix. Indeed, MMP2 is significantly upregulated in activated HSCs during liver fibrosis progression, regulating the degradation of the normal

liver matrix and further promoting LF (Arthur, 2000). Col1 α 1 and MMP2 are primarily produced by HSCs during LF (Barcena-Varela et al., 2019). In this study, the overexpression of miR-654-5p promoted the expression of these fibrogenic genes in LX-2 cells, suggesting that miR-654-5p promotes the progression of LF.

Numerous studies have shown that miRNAs play key roles in HSC activation and LF. For example, miR-188-5p induces the activation and proliferation of HSCs, subsequently aggravating LF (Riaz et al., 2021). Meanwhile, miR-15b and miR-16 limit HSC proliferation and the fibrogenic response (Ma et al., 2021), whereas miR-34c promotes HSC activation and LF (Li et al., 2021c). Additionally, miR-494-3p attenuates HSC activation and induces apoptosis in LF (Li et al., 2021d). Moreover, miR-29a-3p suppresses HSC proliferation by targeting PIK3R3 (Fu et al., 2020).

Several studies have also investigated the effect of RXR α on HSC activation and the regulation of HSC function (Ohata et al., 1997; Vogel et al., 2000; He et al., 2020). RXR α inhibits HSC proliferation (Sharvit et al., 2013) and regulates apoptosis in certain cell types, including pancreatic beta cells (Chen et al., 2019) and mouse hippocampal cells (Litwa et al., 2016).



Therefore, further investigation into RXR α -related regulation of HSCs may provide new perspectives for LF treatment.

Studies have shown that certain miRNAs participate in the LF process by targeting RXR α . For example, miR-34a expression is upregulated in the fibrotic liver, and miR-34a regulates the expression of downstream genes by targeting RXR α (Oda et al., 2014). Moreover, Ji et al. (Ji et al., 2009) found that miR-27a and 27b were upregulated in activated rat HSCs *in vitro*. Meanwhile, transfecting HSCs with anti-miR-27a and anti-miR-27b restored lipid droplets and inhibited the proliferation of HSCs by negatively regulating RXR α . To better understand the biological function of miR-654-5p in LF, we overexpressed miR-654-5p in LX-2 cells, and our *in vitro* results demonstrated that miR-654-5p directly targets RXR α . Moreover, overexpression of miR-654-5p induces HSCs to synthesize collagen by inhibiting RXR α during LF. We also observed a significant increase in miR-654-5p expression and

downregulation of RXR α in the CCl₄-induced fibrosis mouse model. Therefore, collectively these findings suggest that overexpression of miR-654-5p promotes LF progression in mice.

Several limitations were noted in this study. First, in addition to an miR-654-5p mimic, the miR-654-5p inhibitor was also used to treat LX-2 cells in this study. However, owing to the low transcription baseline of miR-654-5p in LX-2 cells, no significant effect was observed on its expression following the use of its inhibitor (this data is not shown in the paper). As an alternative, we overexpressed miR-654-5p in a murine model rather than inhibiting it. Second, α -SMA is a marker of myofibroblasts and is upregulated during HSC activation (myofibroblast-like cells) (Liu et al., 2019). However, in our study, the miR-654-5p mimic did not induce a significant change in the expression of α -SMA in LX-2 cells (data not shown). We speculate that the lack of detectable mRNA responses might be due to characteristics of LX-2, which is an immortalized HSC cell line and can be considered an

activated phenotype of primary HSCs (Xu et al., 2005). In our study, although we controlled for the number of passages of LX-2 (<10), α -SMA mRNA in LX-2 cells had a very high baseline level of α -SMA mRNA, which made it difficult to increase during further activation of LX-2 cells. Furthermore, no significant changes were detected in the expression of α -SMA in LX-2 cells after treatment with TGF- β 1.

In conclusion, the findings of the study show that miR-654-5p induces activation and proliferation of HSCs, while inhibiting their apoptosis. In addition, miR-654-5p aggravates LF by, at least in part, blocking RXR α . Therefore, our findings may provide a new treatment strategy for LF.t

DATA AVAILABILITY STATEMENT

The original contributions presented in the study are included in the article/**Supplementary Material**, further inquiries can be directed to the corresponding authors.

ETHICS STATEMENT

The studies involving human participants were reviewed and approved by ethical committee of the First Hospital of Jilin University. The patients/participants provided their written informed consent to participate in this study.

REFERENCES

- Abdel-Bakky, M. S., Helal, G. K., El-Sayed, E. M., Alhowail, A. H., Mansour, A. M., Alharbi, K. S., et al. (2020). Silencing of Tissue Factor by Antisense Deoxyoligonucleotide Mitigates Thioacetamide-Induced Liver Injury. *Naunyn-schmiedeberg's Arch. Pharmacol.* 393 (10), 1887–1898. PubMed PMID: 32430618. doi:10.1007/s00210-020-01896-0
- Arthur, M. J. P. (2000). Fibrogenesis II. Metalloproteinases and Their Inhibitors in Liver Fibrosis. *Am. J. Physiology-Gastrointestinal Liver Physiol.* 279 (2), G245–G249. PubMed PMID: 10915630. doi:10.1152/ajpgi.2000.279.2.g245
- Barcena-Varela, M., Colyn, L., and Fernandez-Barrena, M. G. (2019). Epigenetic Mechanisms in Hepatic Stellate Cell Activation during Liver Fibrosis and Carcinogenesis. *Ijms* 20 (10), 2507. PubMed PMID: 31117267. doi:10.3390/ijms20102507
- Bataller, R., and Brenner, D. A. (2005). Liver Fibrosis. *J. Clin. Invest.* 115 (2), 209–218. PubMed PMID: 15690074. doi:10.1172/jci24282
- Chen, G., Hu, M., Wang, X. C., Du, S. H., Cheng, Z. X., Xu, J., et al. (2019). Effects of RXR α on Proliferation and Apoptosis of Pancreatic Cancer Cells through TGF- β /Smad Signaling Pathway. *Eur. Rev. Med. Pharmacol. Sci.* 23 (11), 4723–4729. PubMed PMID: 31210298. doi:10.26355/eurrev_201906_18053
- Ezhilarasan, D. (2020). MicroRNA Interplay between Hepatic Stellate Cell Quiescence and Activation. *Eur. J. Pharmacol.* 885, 173507. PubMed PMID: 32858048. doi:10.1016/j.ejphar.2020.173507
- Ezhilarasan, D., Sokal, E., and Najimi, M. (2018). Hepatic Fibrosis: It Is Time to Go with Hepatic Stellate Cell-specific Therapeutic Targets. *Hepatobiliary Pancreat. Dis. Int.* 17 (3), 192–197. PubMed PMID: 29709350. doi:10.1016/j.hbpd.2018.04.003
- Fang, Z., Dou, G., and Wang, L. (2021). MicroRNAs in the Pathogenesis of Nonalcoholic Fatty Liver Disease. *Int. J. Biol. Sci.* 17 (7), 1851–1863. PubMed PMID: 33994867. doi:10.7150/ijbs.59588
- Friedman, S. L. (2008). Mechanisms of Hepatic Fibrogenesis. *Gastroenterology* 134 (6), 1655–1669. PubMed PMID: 18471545. doi:10.1053/j.gastro.2008.03.003

AUTHOR CONTRIBUTIONS

JN and XG conceived of and designed the study. HM performed the experiments, analyzed the data and drafted the manuscript. XW and XL participated in the experiments. CW assisted in sample collection.

FUNDING

The study was sponsored by the National Natural Science Foundation of China (grant No. 81970519 and 81700534) and the WBE Liver Fibrosis Foundation (grant No. CFHPC2022002).

SUPPLEMENTARY MATERIAL

The Supplementary Material for this article can be found online at: <https://www.frontiersin.org/articles/10.3389/fcell.2022.841248/full#supplementary-material>

Supplementary Figure S1 | MiR-654-5p and RXR α expression levels in culture-activated HSCs/quiescent HSCs according to previous RNA-sequencing data. Error bars represent mean \pm SEM of experiments, **p < 0.01, and ***p < 0.001.

Supplementary Figure S2 | The targeting relationship between miR-654-5p and RXR α in human predicted by the Targetscan database.

Supplementary Figure S3 | The targeting relationship between miR-654-5p and RXR α in mouse predicted by the Targetscan database.

- Fu, J., Wu, B., Zhong, S., Deng, W., and Lin, F. (2020). miR-29a-3p Suppresses Hepatic Fibrosis Pathogenesis by Modulating Hepatic Stellate Cell Proliferation via Targeting PIK3R3 Gene Expression. *Biochem. Biophysical Res. Commun.* 529 (4), 922–929. PubMed PMID: 32819600. doi:10.1016/j.bbrc.2020.06.102
- He, L., Yuan, H., Liang, J., Hong, J., and Qu, C. (2020). Expression of Hepatic Stellate Cell Activation-Related Genes in HBV-, HCV-, and Nonalcoholic Fatty Liver Disease-Associated Fibrosis. *PLoS ONE* 15 (5), e0233702. PubMed PMID: 32442221. doi:10.1371/journal.pone.0233702
- Huang, F., Wu, X., Wei, M., Guo, H., Li, H., Shao, Z., et al. (2020). miR-654-5p Targets HAX-1 to Regulate the Malignancy Behaviors of Colorectal Cancer Cells. *Biomed. Res. Int.* 2020, 1–6. PubMed PMID: 32104694. doi:10.1155/2020/4914707
- Ji, J., Zhang, J., Huang, G., Qian, J., Wang, X., and Mei, S. (2009). Over-expressed microRNA-27a and 27b Influence Fat Accumulation and Cell Proliferation during Rat Hepatic Stellate Cell Activation. *FEBS Lett.* 583 (4), 759–766. PubMed PMID: 19185571. doi:10.1016/j.febslet.2009.01.034
- Kong, R. (2020). Circular RNA Hsa_circ_0085131 Is Involved in Cisplatin-resistance of Non-small-cell Lung Cancer Cells by Regulating Autophagy. *Cell Biol Int* 44 (9), 1945–1956. PubMed PMID: 32449799. doi:10.1002/cbin.11401
- Li, B., Cai, S.-Y., and Boyer, J. L. (2021). The Role of the Retinoid Receptor, RAR/RXR Heterodimer, in Liver Physiology. *Biochim. Biophys. Acta (Bba) - Mol. Basis Dis.* 1867 (5), 166085. PubMed PMID: 33497820. doi:10.1016/j.bbadis.2021.166085
- Li, B., Liu, J., Xin, X., Zhang, L., Zhou, J., Xia, C., et al. (2021). MiR-34c Promotes Hepatic Stellate Cell Activation and Liver Fibrogenesis by Suppressing ACSL1 Expression. *Int. J. Med. Sci.* 18 (3), 615–625. PubMed PMID: 33437196. doi:10.7150/ijms.51589
- Li, H., Zhang, L., Cai, N., Zhang, B., and Sun, S. (2021). MicroRNA-494-3p Prevents Liver Fibrosis and Attenuates Hepatic Stellate Cell Activation by Inhibiting Proliferation and Inducing Apoptosis through Targeting TRAF3. *Ann. Hepatol.* 23, 100305. PubMed PMID: 33434689. doi:10.1016/j.aohep.2021.100305
- Li, X., Li, J., Lu, P., and Li, M. (2021). LINC00261 Relieves the Progression of Sepsis-Induced Acute Kidney Injury by Inhibiting NF-Kb Activation through

- Targeting the miR-654-5p/SOCS3 axis. *J. Bioenerg. Biomembr* 53 (2), 129–137. PubMed PMID: 33481135. doi:10.1007/s10863-021-09874-8
- Litwa, E., Rzemieniec, J., Wnuk, A., Lason, W., Krzeptowski, W., and Kajta, M. (2016). RXR α , PXR and CAR Xenobiotic Receptors Mediate the Apoptotic and Neurotoxic Actions of Nonylphenol in Mouse Hippocampal Cells. *J. Steroid Biochem. Mol. Biol.* 156, 43–52. PubMed PMID: 26643981. doi:10.1016/j.jsbmb.2015.11.018
- Liu, H., Zhang, S., Xu, S., Koroleva, M., Small, E. M., and Jin, Z. G. (2019). Myofibroblast-specific YY1 Promotes Liver Fibrosis. *Biochem. Biophysical Res. Commun.* 514 (3), 913–918. PubMed PMID: 31084931. doi:10.1016/j.bbrc.2019.05.004
- Lu, M., Wang, C., Chen, W., Mao, C., and Wang, J. (2018). miR-654-5p Targets GRAP to Promote Proliferation, Metastasis, and Chemoresistance of Oral Squamous Cell Carcinoma through Ras/MAPK Signaling. *DNA Cel Biol.* 37 (4), 381–388. PubMed PMID: 29364705. doi:10.1089/dna.2017.4095
- Lu, Y., Zhang, J., and Wu, Y. (2021). Interference with circRNA DOCK1 Inhibits Hepatocellular Carcinoma Cell Proliferation, Invasion and Migration by Regulating the miR-654-5p/SMAD2 axis. *Mol. Med. Rep.* 24 (2). PubMed PMID: 34184075. doi:10.3892/mmr.2021.12247
- Ma, L., Liu, J., Xiao, E., Ning, H., Li, K., Shang, J., et al. (2021). MiR-15b and miR-16 Suppress TGF- β 1-Induced Proliferation and Fibrogenesis by Regulating LOXL1 in Hepatic Stellate Cells. *Life Sci.* 270, 119144. PubMed PMID: 33545201. doi:10.1016/j.lfs.2021.119144
- Oda, Y., Nakajima, M., Tsuneyama, K., Takamiya, M., Aoki, Y., Fukami, T., et al. (2014). Retinoid X Receptor α in Human Liver Is Regulated by miR-34a. *Biochem. Pharmacol.* 90 (2), c-187. PubMed PMID: 24832862. doi:10.1016/j.bcp.2014.05.002
- Ohata, M., Lin, M., Satre, M., and Tsukamoto, H. (1997). Diminished Retinoic Acid Signaling in Hepatic Stellate Cells in Cholestatic Liver Fibrosis. *Am. J. Physiol.* 272 (3 Pt 1), G589–G596. PubMed PMID: 9124579. doi:10.1152/ajpgi.1997.272.3.G589
- Riaz, F., Chen, Q., Lu, K., Osoro, E. K., Wu, L., Feng, L., et al. (2021). Inhibition of miR-188-5p Alleviates Hepatic Fibrosis by Significantly Reducing the Activation and Proliferation of HSCs through PTEN/PI3K/AKT Pathway. *J. Cel Mol Med* 25 (8), 4073–4087. PubMed PMID: 33689215. doi:10.1111/jcmm.16376
- Roeb, E. (2018). Matrix Metalloproteinases and Liver Fibrosis (Translational Aspects). *Matrix Biol.* 68–69, 463–473. PubMed PMID: 29289644. doi:10.1016/j.matbio.2017.12.012
- Sharvit, E., Abramovitch, S., Reif, S., and Bruck, R. (2013). Amplified Inhibition of Stellate Cell Activation Pathways by PPAR- γ , RAR and RXR Agonists. *PLoS ONE* 8 (10), e76541. PubMed PMID: 24098526. doi:10.1371/journal.pone.0076541
- Tan, Y. Y., Xu, X. Y., Wang, J. F., Zhang, C. W., and Zhang, S. C. (2016). MiR-654-5p Attenuates Breast Cancer Progression by Targeting EPST11. *Am. J. Cancer Res.* 6 (2), 522–532. PubMed PMID: 27186421.
- Tao, Y., Wang, N., Qiu, T., and Sun, X. (2020). The Role of Autophagy and NLRP3 Inflammasome in Liver Fibrosis. *Biomed. Res. Int.* 2020, 1–8. PubMed PMID: 32733951. doi:10.1155/2020/7269150
- Tsai, L. M., and Yu, D. (2010). MicroRNAs in Common Diseases and Potential Therapeutic Applications. *Clin. Exp. Pharmacol. Physiol.* 37 (1), 102–107. PubMed PMID: 19671070. doi:10.1111/j.1440-1681.2009.05269.x
- Tsuchida, T., and Friedman, S. L. (2017). Mechanisms of Hepatic Stellate Cell Activation. *Nat. Rev. Gastroenterol. Hepatol.* 14 (7), 397–411. PubMed PMID: 28487545. doi:10.1038/nrgastro.2017.38
- Vogel, S., Piantedosi, R., Frank, J., Lalazar, A., Rockey, D. C., Friedman, S. L., et al. (2000). An Immortalized Rat Liver Stellate Cell Line (HSC-T6): a New Cell Model for the Study of Retinoid Metabolism *In Vitro*. *J. Lipid Res.* 41 (6), 882–893. PubMed PMID: 10828080. doi:10.1016/s0022-2275(20)32030-7
- Wang, S., Guo, Y., Zhang, X., and Wang, C. (2021). miR-654-5p Inhibits A-utophagy by T-targeting ATG7 via mTOR S-signaling in I-ntervertebral D-isc D-egeneration. *Mol. Med. Rep.* 23 (6), 12083. PubMed PMID: 33846806. doi:10.3892/mmr.2021.12083
- Wang, Z., Xu, J., Zheng, Y., Chen, W., Sun, Y., Wu, Z., et al. (2011). Effect of the Regulation of Retinoid X Receptor- α Gene Expression on Rat Hepatic Fibrosis. *Hepatol. Res.* 41 (5), 475–483. PubMed PMID: 21518404. doi:10.1111/j.1872-034X.2011.00794.x
- Werner, M., Driftmann, S., Kleinehr, K., Kaiser, G. M., Mathé, Z., Treckmann, J.-W., et al. (2015). All-In-One: Advanced Preparation of Human Parenchymal and Non-parenchymal Liver Cells. *PLoS ONE* 10 (9), e0138655. PubMed PMID: 26407160. doi:10.1371/journal.pone.0138655
- Xu, L., Hui, A. Y., Albanis, E., Arthur, M. J., O'Byrne, S. M., Blaner, W. S., et al. (2005). Human Hepatic Stellate Cell Lines, LX-1 and LX-2: New Tools for Analysis of Hepatic Fibrosis. *Gut* 54 (1), 142–151. PubMed PMID: 15591520. doi:10.1136/gut.2004.042127
- Xu, X. Z., Song, H., Zhao, Y., and Zhang, L. (2020). MiR-654-5p Regulated Cell Progression and Tumor Growth through Targeting SIRT6 in Osteosarcoma. *Eur. Rev. Med. Pharmacol. Sci.* 24 (7), 3517–3525. PubMed PMID: 32329825. doi:10.26355/eurrev_202004_20811
- Zhang, J., Furuta, T., Sabit, H., Tamai, S., Jiapaer, S., Dong, Y., et al. (2020). Gelsolin Inhibits Malignant Phenotype of Glioblastoma and Is Regulated by miR-654-5p and miR-450b-5p. *Cancer Sci.* 111 (7), 2413–2422. PubMed PMID: 32324311. doi:10.1111/cas.14429

Conflict of Interest: The authors declare that the research was conducted in the absence of any commercial or financial relationships that could be construed as a potential conflict of interest.

Publisher's Note: All claims expressed in this article are solely those of the authors and do not necessarily represent those of their affiliated organizations, or those of the publisher, the editors and the reviewers. Any product that may be evaluated in this article, or claim that may be made by its manufacturer, is not guaranteed or endorsed by the publisher.

Copyright © 2022 Ma, Wang, Liu, Wang, Gao and Niu. This is an open-access article distributed under the terms of the Creative Commons Attribution License (CC BY). The use, distribution or reproduction in other forums is permitted, provided the original author(s) and the copyright owner(s) are credited and that the original publication in this journal is cited, in accordance with accepted academic practice. No use, distribution or reproduction is permitted which does not comply with these terms.